

Physicochemical Properties and Microstructure Formation of the Surfactant Mixtures of Sodium *N*-(2-(*n*-Dodecylamino)ethanoyl)-L-alaninate and SDS in Aqueous Solutions

Dibyendu Khatua,[†] Sampad Ghosh,[†] Joykrishna Dey,^{*,†} Goutam Ghosh,[‡] and V. K. Aswal[§]

Department of Chemistry, Indian Institute of Technology, Kharagpur 721 302, India, and UGC-DAE Consortium for Scientific Research and Solid State Physics Division, BARC, Trombay, Mumbai 400 085, India

Received: October 3, 2007; In Final Form: February 1, 2008

Aggregation behavior of a novel anionic amphiphilic molecule, sodium *N*-(2-(*n*-dodecylamino)ethanoyl)-L-alaninate (C₁₂Ala), was studied in the presence of sodium dodecyl sulfate (SDS) surfactant at different [C₁₂-Ala]/[SDS] molar ratios and concentrations. The viscosity of aqueous SDS solution increased in the presence of C₁₂Ala surfactant. The bulk viscosity of water was found to increase upon increase of both molar ratio and total surfactant concentration. The microenvironments of the self-assemblies were investigated using the fluorescence probe technique. Fluorescence anisotropy studies indicated formation of rodlike micelles. Both dynamic light scattering and small-angle neutron scattering measurements were performed to obtain the size and shape of the microstructures. The concentration and composition dependence of the hydrodynamic diameter of the aggregates were investigated. Transmission electron micrographs revealed the presence of a hexagonal liquid crystal phase in dilute solutions of the C₁₂Ala–SDS mixture. The micrographs of moderately concentrated solution, however, showed cholesteric liquid-crystal structures with fingerprint-like texture. Temperature-dependent phase behavior of the self-assemblies was studied by use of the fluorescence probe technique.

Introduction

The micelles composed of mixed surfactants occurring in biological fluids are very often preferred in industrial preparations and pharmaceutical and medicinal formulations for the purpose of solubilization, suspension, dispersion, etc.^{1–3} In fact, mixed surfactants are used in most practical applications rather than individual surfactants. Solubilization behavior of different compounds in the mixed micellar solution of cationic surfactants has been studied by several researchers.^{4–6} There are many reports in the literature on studies of different combination of mixed surfactant system viz. cationic–cationic,⁷ nonionic–nonionic,^{7,8} anionic–cationic,⁹ anionic–nonionic,^{10,11} etc. Although many mixed surfactant systems have been extensively studied, there are fewer studies on the ion pair surfactants,^{12,13} since the latter are insoluble in water. Recently, studies related to the formation and subsequent growth of vesicles using mixed surfactants of anionic sodium octyl sulfate (SOS) and cationic cetyltrimethylammonium bromide (CTAB) have been reported.^{14–17} Currently “catanionic” (mixtures of cationic and anionic surfactants) surfactants have attracted tremendous attention because they form stable unilamellar vesicles in dilute cation- or anion-rich solutions.^{18–21} At higher concentrations, however, mixed micelles with wormlike morphologies are usually observed. On the other hand, at higher molar ratios, the catanionic systems always produce rod- or wormlike micelles at all concentrations as indicated by the increase of bulk solution viscosity. The rheological behavior of such surfactant solutions has been reported.^{22,23}

Although there are a handful of studies on catanionic surfactant systems, fewer studies have been done on the mixtures

of anionic and zwitterionic surfactants.^{24–26} Recently, we have observed that, in acidic medium, sodium *N*-(2-(*n*-dodecylamino)ethanoyl)-L-valinate (C₁₂Val) in the presence of SDS gels water.²⁷ However, the corresponding L-alanine (C₁₂Ala) and glycine (C₁₂Gly) derivatives failed to gel water under similar conditions but resulted in the formation of viscous solution at neutral pH. This led us to investigate the aggregation behavior of these mixed-surfactant systems. These surfactants exist in the zwitterionic form at neutral pH. Thus, in the presence of SDS a 1:1 complexation can give rise to produce a double-tailed anionic surfactant with the polar amino acid as headgroup (see Figure 1 for structure). In this study, an effort has been made to understand the aggregation behavior of the mixtures of C₁₂Ala and SDS surfactants at different molar ratios as well as at different concentrations. The self-assembly formation has been studied by use of a number of techniques, such as surface tension, fluorescence probe, dynamic light scattering, small-angle neutron scattering, and electron microscopy.

Experimental Section

Materials. The amphiphile C₁₂Ala was synthesized and purified according to the procedure reported elsewhere.²⁷ The compound was chemically identified by ¹H and ¹³C NMR, IR spectra, and elemental analysis. Optical purity was determined by measurement of specific rotation. The fluorescence probes pyrene, *N*-phenyl-1-naphthylamine (NPN), 1,6-diphenyl-1,3,5-hexatriene (DPH), and SDS were procured from Aldrich and were purified by recrystallization from an acetone–ethanol mixture. The purity of the probes was confirmed by measurement of fluorescence excitation spectra. Doubly distilled water was used for solution preparation.

Methods. The ¹H NMR spectra were recorded on a Bruker 400 MHz spectrometer. UV–visible spectra were recorded on a Shimadzu (model 1601) spectrophotometer. The surface tension measurements were performed with a Torsion Balance

* To whom correspondence should be addressed. E-mail: joydey@chem.iitkgp.ernet.in. Phone: 91-3222-283308. Fax: 91-3222-255303.

[†] Indian Institute of Technology.

[‡] UGC-DAE Consortium for Scientific Research, BARC.

[§] Solid State Physics Division, BARC.

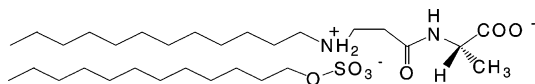


Figure 1. Chemical structure of the C₁₂Ala–SDS complex.

(S.D. Hurdson & Co., Kolkata, India) by using a Du Nüoy ring detachment method. Bulk viscosity of surfactant solutions were measured with a Brookfield rotational viscometer (model DV-III) using cone–plate geometry. A Thermo Orion model 710A+ digital pH meter was used to measure the pH of the solutions. Temperature-controlled measurements were carried out by use of a Thermo Neslab RTE-7 circulating bath.

The surfactants were mixed in a volumetric flask in desired molar ratios using appropriate volumes of respective stock solution (100 mM) in methanol. The solvent was dried in water bath. This ensured ion-pairing at the >NH₂⁺ group of C₁₂Ala. This was confirmed further by the upfield shift of the >NH₂⁺ proton signal (which normally appears in the range $\delta \sim 8.5$ – 6.0)²⁸ to $\delta \sim 3.3$ – 3.1 in the ¹H NMR spectrum (see Figure S1 of the Supporting Information) of the 1:1 mixture. To the dry mass thus obtained an appropriate volume of double distilled water was added to obtain surfactant solution of known concentration. The C₁₂Ala–SDS mixtures with *R* in the range of 0.2–1.5 were observed to be soluble at all concentrations. The solubility of the 1:1 mixture in the concentration range employed also suggests that C₁₂Ala is present completely in the ion-pair state as shown in Figure 1. The pH of the dilute aqueous solutions of C₁₂Ala–SDS mixtures with *R* in the range of 0.2–1.5 was observed to be ~ 6.8 .

Saturated aqueous solutions of NPN and pyrene were used for sample preparation. Since DPH is insoluble in water, a 1.0 mM stock solution of the probe in 20% (v/v) methanol–water mixture was prepared. The final concentration of the probe was adjusted to 1.0 μ M by addition of an appropriate amount of the stock solution.

Steady-state fluorescence spectra of pyrene were recorded with a SPEX FL 3-11 spectrofluorometer. The emission spectra of NPN and DPH, on the other hand, were measured with a Perkin-Elmer LS-55 luminescence spectrometer equipped with filter polarizers that use the L-format configuration. A quartz cell of 1-cm path length was used for all fluorescence measurements. The samples containing pyrene were excited at 335 nm using excitation and emission slits with bandpass 2 and 1.0 nm, respectively. On the other hand, the samples containing DPH and NPN were excited at 350 nm and the emission intensity was measured in the range 360–560 nm. The excitation slit with bandpass of 2.5 nm and the emission slit with bandpass between 2.5 and 7.5 nm were used the measurements. All spectra were blank subtracted. The anisotropy measurements were carried out by use of an LS-55 luminescence spectrometer. The fluorescence intensity was monitored at 450 nm, and a 430 nm cutoff filter was placed in the emission beam to eliminate the effects of scattered radiation. An average of six measurements was always recorded. Unless otherwise mentioned, the temperature of all experiments was kept at 30 ± 0.5 °C.

Time-resolved fluorescence intensity decay was measured by the time-correlated single-photon counting method using a picosecond diode laser ($\lambda = 370$ nm, IBH, Glasgow, U.K., nanoLED-03) as a source for excitation. The typical response time of the laser was 70 ps. Fluorescence lifetimes were obtained from analysis the decays using IBH DAS-6 multiexponential decay analysis software. Best fitting was judged from the χ^2 value (0.9–1.3) and from randomness of the residual plot.

The DLS measurements were carried out by a home-built spectrometer the details of which are available elsewhere.²⁹ A

TABLE 1: Critical Aggregation Concentration (cac), γ_{cac} , pC_{20} , cac/C_{20} , and Micropolarity (I_1/I_3) Values of Various Compositions of C₁₂Ala–SDS Mixtures (2 mM) at 30 °C^a

composn	cac (mM)	γ_{cac} (mN/m)	pC_{20}	cac/C_{20}	I_1/I_3
3:2	0.40 (0.37)	26.0	4.30	8.08	1.12
1:1	0.35 (0.29)	23.0	4.47	10.2	1.12
1:2	0.37 (0.32)	21.9	4.00	3.70	1.12
1:4	0.45 (0.50)	22.4	4.35	9.22	1.11
1:5	0.61 (0.65)	21.4	3.85	4.30	1.09

^a Values within parentheses were obtained from fluorescence measurements.

15-mW He–Ne laser ($\lambda_0 = 632.8$ nm) was used for the measurement. The scattering radiation was measured at 90° to the incident beam. The intensity autocorrelation functions were analyzed using the cumulant method.³⁰

Small-angle neutron scattering measurements were performed using a SANS diffractometer at Dhruva reactor, BARC, Mumbai, India.³¹ The diffractometer makes use of a BeO filter which provides mean a wavelength of neutrons 5.2 Å with a wavelength resolution of 15%. A one-dimensional position sensitive detector was used for recording the angular distribution of scattered neutrons. The range of wave vector transfer ($Q = 4\pi \sin \theta/\lambda$), where the wavelength of the incident neutron is λ (5.2 Å) and 2θ is the scattering angle, was 0.018–0.30 Å^{−1}. A UV grade quartz sample cell of path length 5 mm was used for the measurements. The measured scattering intensities of neutrons were corrected for background and empty cell scattering and sample transmission. The intensities were normalized to absolute cross section units, and plots of coherent differential cross section ($d\Sigma/d\Omega$) versus Q were obtained. The prolate ellipsoidal ($a \neq b = c$) shape of the micelles was used in the analysis of SANS data. The parameters in the analysis were optimized by means of a nonlinear least-square fitting program. The aggregation number (N) was calculated from the relation $N = 4\pi ab^2/3v$, where v is the volume of the surfactant monomer. The uncertainty in the scattered data was estimated to be <10%.

Electron micrographs were obtained with a JEOL-JEM 2100 Japan transmission electron microscope operating at an accelerating voltage of 200 kV at room temperature. A 5 μ L volume of solution was placed on a 400 mesh size carbon-coated copper grid, allowed to adsorb for 1 min, blotted with filter paper, air-dried, and then negatively stained with freshly prepared 1.5% aqueous uranyl acetate. The specimens were kept in desiccators before use.

Results and Discussion

Surface Tension Studies. The critical aggregation concentration (cac) values of C₁₂Ala–SDS mixtures for various compositions were determined by surface tension measurements. The cac values thus obtained for different compositions are listed in Table 1 along with other surface properties. The cac value increases slightly as the molar ratio decreases. It is important to note that the cac values of the mixtures are much less than that of pure SDS (8.0 mM) in water and pure C₁₂Ala (0.6 mM) in alkaline solution (see Supporting Information). Such a large decrease of cac of SDS can be explained by the formation of mixed micelles containing 1:1 ion-pair complex (Figure 1) and SDS surfactant. The ion-pair complex may be considered as a double chain carboxylate surfactant. Thus, strong hydrophobic interaction among hydrocarbon chains of the constituent surfactants results in a lower cac value. The increase of cac with the decrease of molar ratio is due to the increased electrostatic repulsion between surfactant headgroups as a consequence of

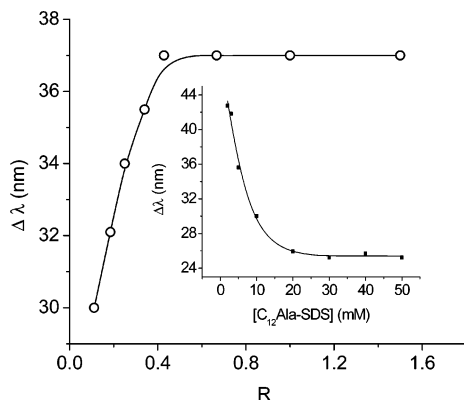


Figure 2. Wavelength shift ($\Delta\lambda$) of NPN in the presence of 10 mM $C_{12}Ala$ -SDS mixture at different ratios (R). Inset: Plot of $\Delta\lambda$ as a function of $[C_{12}Ala-SDS]$ for 1:5 mixtures.

gradual incorporation of more SDS surfactants in the mixed micelle.

The mixed-surfactant systems have very good surface activity compared to pure SDS surfactant as indicated by the respective γ_{cac} , pC_{20} (negative logarithm of surfactant concentration at which the surface tension of water is reduced by 20 units), and cac/C_{20} . The pC_{20} values of all the surfactant mixtures are greater than 3.0, which suggest that they are good surface-active agents.³² The data in Table 1 show that the surface activity is highest when the surfactants are present in equimolar quantities. The large hydrophobic volume of the ion-pair complex is responsible for the higher surface activity. The surface activity decreases with either increase or decrease of SDS content of the mixtures. For all the surfactant mixtures, the tendency of surface adsorption is higher as compared to micelle formation in the bulk water. This is indicated by the cac/C_{20} (>1.0) values.

Fluorescence Probe Studies. The cac values were also determined by fluorescence titration method using NPN as fluorescent probe. Though NPN is weakly fluorescent in aqueous solution, its fluorescence spectrum in nonpolar solvent shows a huge increase in intensity accompanied by a large spectral shift toward shorter wavelength relative to that in water.³³ The NPN probe also exhibits enhancement of fluorescence intensity and blue shift of the position of emission maximum upon its solubilization near the headgroup region of micelles. In other words, the NPN probe reports the polarity of the microenvironment. The NPN fluorescence was therefore measured in the presence of different concentrations of $C_{12}Ala$ -SDS mixtures. The cac values obtained from the inflection points of the plots (not shown) of relative intensity versus surfactant concentration are included in Table 1. The data show that the cac values obtained by the two methods, within the experimental error, are almost equal. The large blue shift, $\Delta\lambda$ ($=\lambda_{water} - \lambda_{surf}$), of the emission spectrum of NPN (not shown) at a total surfactant concentration above cac value of $C_{12}Ala$ -SDS mixture indicates solubilization of the probe molecules within domains much less polar than water. The $\Delta\lambda$ value, however, was observed to increase (Figure 2) asymptotically when the molar ratio of the amphiphiles in the mixture increased at a given concentration greater than the cac value. This is due to the incorporation of more $C_{12}Ala$ -containing hydrophobic headgroup in the micelle interface that results in a reduction of electrostatic repulsion between headgroups of SDS surfactant. This has been further substantiated by the lower values of polarity ratio, I_1/I_3 , of pyrene probe, which measures micropolarity of the micelle core-headgroup interface.^{34,35} The relevant data are compiled in Table 1. It can be observed that the values of I_1/I_3 are much smaller

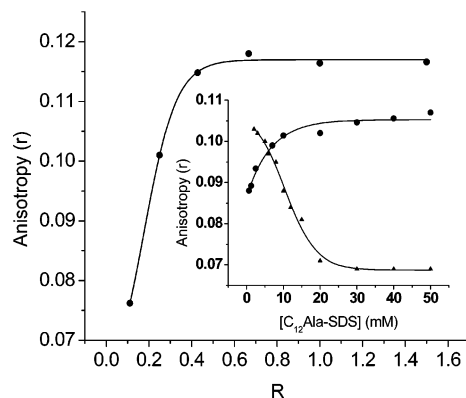


Figure 3. Change of fluorescence anisotropy (r) of the DPH probe as a function of molar ratio (R) of the $C_{12}Ala$ -SDS mixture (10 mM). Inset: Plot of r versus $[C_{12}Ala-SDS]$ for 1:1 (●) and 1:5 (▲) mixtures.

relative than that in water (1.71), suggesting that the microenvironments of pyrene molecules are much less polar than bulk water. It is important to note that the I_1/I_3 index values are also lower than that of normal micelles of ionic surfactants for which the I_1/I_3 value is typically ~ 1.40 .¹ It is observed that unlike the $\Delta\lambda$ value the I_1/I_3 index is independent of composition of the mixture. These observations suggest (i) stronger hydrophobic interaction among hydrocarbon chains of the aggregates which expels water from the headgroup region and (ii) solubilization of the pyrene molecules in the more fluid hydrocarbon core of the aggregates. This means that pyrene and NPN probes report the micropolarity of different regions of the aggregates. Although the micropolarity near the headgroup region decreases as a result of expulsion of water molecules, the micropolarity of the hydrocarbon core of the aggregates does not change significantly.

The position of fluorescence maximum of NPN was also measured at different concentrations of the $C_{12}Ala$ -SDS mixture at molar ratios R equal to 1.0 and 0.2. The measurements at $R = 1.0$ showed no significant change. In contrast, the solutions of $R = 0.2$ showed a gradual decrease of $\Delta\lambda$ value with the increase of total surfactant concentration. The data are presented in the plot shown as the inset of Figure 2. The small but significant decrease of $\Delta\lambda$ value suggests a decrease of micropolarity of the aggregates. The decrease of $\Delta\lambda$ with surfactant concentration might be due to transformation of large aggregates to smaller micellar structures whose interfacial region is more polar and less viscous. This is also indicated by the fluorescence anisotropy measurements of DPH probe discussed below.

To further investigate the microenvironments of the aggregates formed, we have measured fluorescence anisotropy of DPH probe in aqueous mixtures of $C_{12}Ala$ and SDS surfactants. In fact, DPH is a well-known membrane fluidity probe and has been used for studying many lipid bilayer membranes.^{36,37} Accordingly, the r -value was measured for different compositions of surfactant mixtures at a concentration above their respective cac values. The relevant data are plotted in Figure 3. As observed, the anisotropy value increases with the increase of molar ratio and is consistent with the increase of $\Delta\lambda$ value as shown in Figure 2. We have also measured the variation of fluorescence anisotropy of DPH probe as a function of total surfactant concentration for two different molar ratios, 1.0 and 0.2. The data are presented in the plots as shown in the inset of Figure 3. It is interesting to observe that upon increase of total surfactant concentration the r -value increases and decreases respectively in the cases of $R = 1.0$ and $R = 0.2$. The small increase of r -value with the increase of molar ratio and

TABLE 2: Fluorescence Lifetime (τ_f), Preexponential Factors (a), χ^2 , Fluorescence Anisotropy (r), and Microviscosity (η_m) of DPH Probe in the Self-Assemblies of C₁₂Ala–SDS Complex ($R = 1$) at 30 °C

concn (mM)	τ_f (ns)	a	χ^2	r	η_m^a (mPa s)
0.77	7.76	1.0	1.196	0.088	33.3
1.9	8.52	1.0	1.228	0.092	38.7
3.85	1.72	0.167	1.174	0.095	41.8
		8.8	0.833		
7.7	1.28	0.199	1.254	0.099	44.8
		8.93	0.801		

^a Values were calculated using the longer lifetime component of DPH fluorescence.

concentration (for $R = 1.0$) might be due to concentration-dependent growth of the aggregates. On the other hand, the decrease of r -value in the case of $R = 0.2$ is indicative of transformation of large aggregates into small micellar aggregates as discussed in the preceding paragraph. In fact, transformation of large vesicles to small micelles with the increase of surfactant concentration in the cationic or anionic rich regions of the mixtures of cationic and anionic surfactants has been reported in the literature.^{18–24}

To estimate the packing of hydrocarbon chains in the interfacial region of the aggregates, we have measured microviscosity (η_m) at different concentrations of the C₁₂Ala–SDS ($R = 1.0$) system from measured fluorescence anisotropy and lifetime (τ_f) values (Table 2) using the method reported in the literature.³⁸ The anisotropy values and hence the η_m values are higher than that of spherical micelles but less than that of bilayer aggregates.^{38,39} It is important to note that there is a significant increase of η_m value with the increase of concentration of surfactant mixture indicating growth of the aggregates in the C₁₂Ala–SDS system in the concentration range examined. This implies formation of either rodlike or flexible wormlike micelles in solutions of the C₁₂Ala–SDS system. The formation of wormlike micelles as indicated by the relatively lower fluorescence anisotropy and microviscosity values is manifested by the higher bulk viscosity of the solution as discussed below. However, the viscosity of the surfactant solutions decreased when heated at higher temperature which might be indicative of a phase change from flexible wormlike micelles to small spherical or rodlike micelles. To investigate how the microstructure changes with the increase of temperature, the fluorescence anisotropy of the DPH probe was measured at different temperatures in the range 20–60 °C in the presence of the C₁₂Ala–SDS mixtures. The corresponding plot is depicted in Figure 4. As seen, the r -value is higher at low temperature, which decreases exponentially with the rise in temperature. It should be noted here that in the absence of C₁₂Ala–SDS mixtures the fluorescence intensity as well as the r -value of the DPH probe, as expected, is very small (<0.05) and showed only a small decrease with the rise of temperature to 60 °C. Therefore, the lowering of the r -value in the presence of C₁₂Ala–SDS mixtures with the increase of temperature must be due to changes in the microstructures of the aggregates in solution. It appears that the large rodlike micelles that exist at room temperature perhaps disintegrate to produce smaller aggregates. Indeed the lower r -value at 60 °C corresponds to the value of small micellar aggregates the microenvironment of which is more fluid in nature.^{36–39}

Small-Angle Neutron Scattering Studies. To examine the shape of the aggregates formed at higher temperatures, we performed SANS measurements. The viscous solution was heated first to 50 °C, and scattered intensity was then measured.

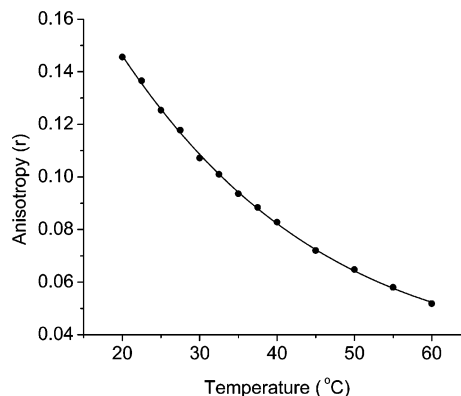


Figure 4. Variation of fluorescence anisotropy (r) of DPH in the presence of a C₁₂Ala–SDS mixture ($R = 1$, $C = 50$ mM) with temperature.

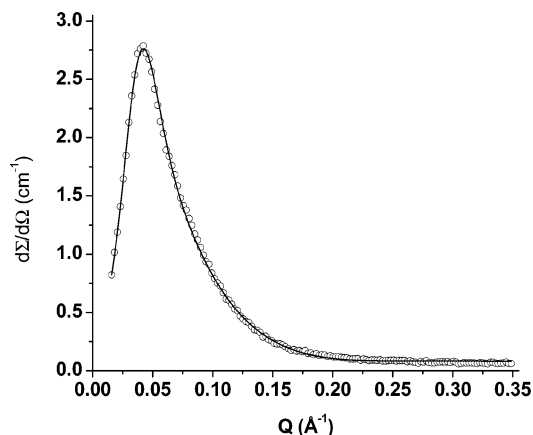


Figure 5. Plot of scattering intensity ($d\Sigma/d\Omega$) versus scattering vector (Q) for C₁₂Ala–SDS ($R = 1.0$, $C = 50$ mM) at 50 °C.

The plots of the measured scattering intensity ($d\Sigma/d\Omega$) versus scattering vector (Q) are shown in Figure 5. The scattering profile is given by the product of the form factor and the structure factor. The form factor depends on the shape and size of the micelles, and the structure factor is decided by the interaction between the micelles. The scattering data for the mixed amphiphile system were best fit to the form factor of an aggregate of cylindrical (ellipsoidal) shape. The structure factor was calculated using the modified Hayter–Penfold type analysis⁴⁰ that considers micelles to be rigid equivalent spheres interacting through screened Coulomb potentials between the charged mixed micelles under a mean spherical approximation. The semimajor (a) and semiminor (b) axes of the aggregates thus obtained are respectively 5.07 and 1.8 nm. The values of aggregation number (N_{agg}) and degree of counterion binding (β) were found to be 163 and 0.9, respectively. The β -value is very large compared to that for micellar aggregates and is consistent with the rodlike micelles. The calculated value of b is closely equal to the hydrocarbon chain length of the amphiphiles. The calculated N_{agg} value is also consistent with the micelle size. Thus, it is confirmed that large wormlike micelles that exist at room temperature are transformed into small rodlike micelles upon heating. In other words, the large wormlike micelles are formed as a result of growth of rodlike micelles with the increase of concentration and with the decrease of temperature.

Viscosity of the Surfactant Solutions. As mentioned earlier, it was observed that the bulk viscosity of water increased upon increase of concentration of the surfactant mixture. In fact, the rise of bulk viscosity of the surfactant solutions was also

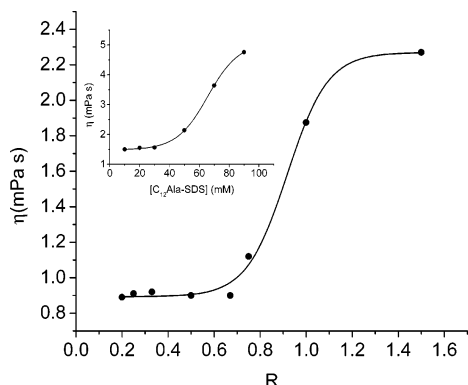


Figure 6. Plot of η (mPa s) versus molar ratio, R , at a given concentration (50 mM) of $C_{12}Ala-SDS$ mixture. Inset: Plot of η (mPa s) versus $[C_{12}Ala-SDS]$ (mM) at a molar ratio of $R = 1.0$.

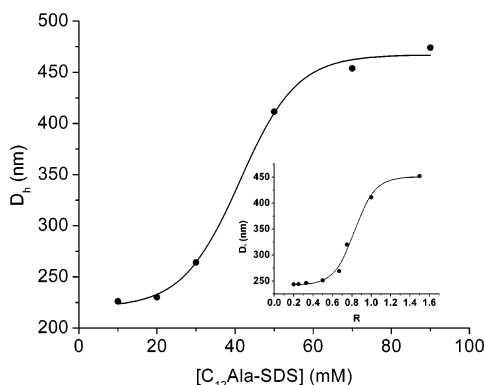


Figure 7. Concentration ($R = 1.0$) and composition (inset; $C = 50$ mM) dependence of hydrodynamic diameter, D_h , of a $C_{12}Ala-SDS$ mixture.

observed when molar ratio of the surfactants in the mixture at a particular concentration was increased. The viscosity change of the solution was therefore systematically studied in the presence of surfactant mixtures. The plots in Figure 6 show the variation of bulk viscosity as a function of $[C_{12}Ala-SDS]$ and molar ratio (R). It is observed that bulk viscosity of the solution increases with the increase of both $[C_{12}Ala-SDS]$ and R . It has been reported in the literature that increase of viscosity of surfactant solution is due to the formation of rodlike micelles.^{41–45} It has also been shown that enhancement of viscosity is proportional to the size of the rodlike micelles. Surfactant solutions containing long threadlike micelles have higher viscosity because of entanglement of the micelles. Thus, wormlike micelles are like polymers with the exception that micelles are in dynamic equilibrium with their monomers. The average micellar length is a thermodynamic quantity, and it responds to changes in solution composition and temperature. Normally, micellar length decreases exponentially with the rise in temperature, which means an exponential decrease of solution viscosity. The existence of large aggregates in aqueous solutions of $C_{12}Ala-SDS$ mixtures was confirmed by the results of DLS studies.

Hydrodynamic Diameter of the Aggregates. To measure the size of the aggregates formed by the surfactant mixtures, the hydrodynamic diameter (D_h) of the aggregates was measured by use of DLS technique at different concentrations and compositions of the $C_{12}Ala-SDS$ mixtures. The $C_{12}Ala-SDS$ mixtures with $R = 1.0$ exhibit monomodal size distributions (not shown). The plots in Figure 7 show the variation of hydrodynamic diameter as a function of $[C_{12}Ala-SDS]$ for a given composition ($R = 1.0$) and as a function of composition

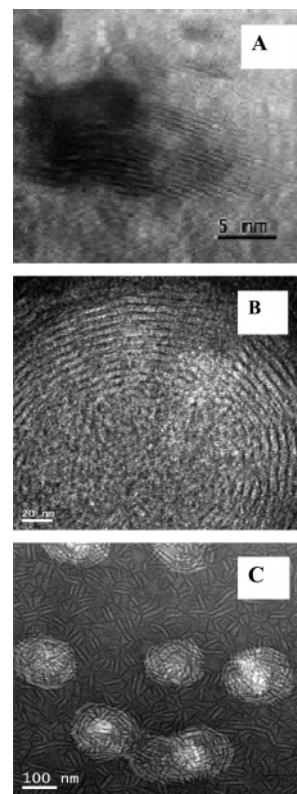


Figure 8. Negatively stained TEM micrographs of (A) 2 mM (1:1), (B) 10 mM (1:1), and (C) 0.8 mM (1:5) $C_{12}Ala-SDS$ mixtures.

for a given concentration (50 mM). The size of the aggregates formed by the surfactant mixtures is very large. It is observed that the average hydrodynamic diameter of the aggregates increases with concentration as well as with the increase of molar ratio, which is consistent with the increase of bulk viscosity of the solution as discussed above. This means that the large aggregates formed by the $C_{12}Ala-SDS$ mixtures are wormlike micelles. Although the size of the rodlike micelles is large, the viscosity of the solutions is relatively low. This might be due to the fact that they are not entangled with each other which causes rise of bulk viscosity.

Microstructures of the Aggregates. Negatively stained TEM micrographs were obtained for both dilute and concentrated solutions of the surfactant mixtures at different molar ratios. However, in the TEM pictures at higher concentrations (> 10 mM) although long rodlike micellar aggregates were seen, due to overloading of samples the clarity was lost. Therefore, we present in Figure 8 the micrographs of only dilute (2 mM) and semidilute (10 mM) solutions of a $C_{12}Ala-SDS$ mixture ($R = 1.0$). The image A clearly shows cylinders packed in a hexagonal array and observed normal to the cylinder axes. The cylinders with their axes arranged parallel to as well as normal to the plane of the grid are seen. The image provides direct evidence of the columnar hexagonal arrangement of these cylindrical micelles in dilute solutions. The image B shown in Figure 8 reveals the presence of a fingerprint-like structure with circular cylinders in semidilute solutions.⁴⁶ The TEM picture clearly suggests that small rodlike micelles that are formed in dilute solutions probably transform into long threads. The formation of rodlike micelles is also evidenced by the micrograph (picture C) of the dilute solution of $C_{12}Ala-SDS$ mixtures with $R = 0.2$. The picture clearly shows the existence of rodlike micelles of width equal to the length of hydrocarbon chain length (~ 2 nm). For the mixtures of $R = 0.2$, no recognizable structures could be observed at higher concentrations (> 10 mM). This

might be because of smaller size of the aggregates as indicated by the results from fluorescence measurements discussed above. The apparent high viscosity of the isotropic solution of 1:1 mixtures is consistent with the formation of wormlike micelles in concentrated solutions. However, no entanglement of the wormlike micelles can be observed. This is consistent with relatively lower viscosity of the mixtures. Although the length of the wormlike micelles could not be precisely measured, the large size of the aggregates is consistent with the corresponding values of D_h obtained by DLS measurements.

A closer look at the structures shows that the wormlike micelles are highly ordered. The average distance between two adjacent threads is about 7 nm. The characteristic fingerprint texture is due to chiral nematic (cholesteric) liquid-crystalline phase. Others have also reported fingerprint-like texture in different surfactant systems.^{47–50} However, the mechanism for the generation of cholesteric behavior of lyotropic liquid-crystalline systems is not well understood. Two basic mechanisms for this behavior have been proposed.^{4,5} The first involves pairwise interactions between chiral centers on adjacent micelles, which is rejected by researchers^{10,11} because such structures could also be found with achiral surfactants. The second mechanism suggests that the presence of chiral centers in the micelle induce distortion in the micelle to give a chiral shape. Interactions between chiral micelles then lead to cholesteric behavior.^{7,11} Since one of the constituent surfactants is chiral, an asymmetry in the interactive forces is obtained. Consequently, information concerning chirality is transmitted via the intermolecular forces and the preferred direction of orientation undergoes a spontaneous twist resulting in the characteristic fingerprint pattern as seen under the microscope.

Conclusions

In conclusion, we have synthesized the novel amino acid-derived surfactant sodium *N*-(2-(*n*-dodecylamino)ethanoyl)-L-alaninate (C₁₂Ala) which upon mixing with SDS surfactant produced isotropic viscous solutions in water at higher total surfactant concentrations. The bulk viscosity of water was found to increase upon increase of both molar ratio and total surfactant concentration. Relatively lower values of fluorescence anisotropy of DPH probe and microviscosity indicated formation of small rodlike and wormlike micelles respectively in dilute and concentrated solutions. DLS measurements confirmed the presence of aggregates of large size in concentrated solutions. The average hydrodynamic diameter of the aggregates was observed to increase with the increase of total concentration and [C₁₂Ala]/[SDS] ratio. Transmission electron micrographs revealed presence of rodlike micelles in dilute solutions of the C₁₂Ala–SDS complex. On the other hand, the micrographs of semidilute solution showed cholesteric liquid-crystal structures with fingerprint-like texture. SANS measurements confirmed that the cholesteric liquid-crystal structure of the aggregates is formed by growth of small rodlike micelles.

Acknowledgment. This work was supported by the DST (Grant No. SR/S1/PC-18/2005), New Delhi. D.K. thanks the CSIR for a senior research fellowship (9/81(524)/2005-EMR-I). We are thankful to Dr. N. Chattopadhyay, Jadavpur University, Kolkata, India, for his assistance with the time-resolved fluorescence measurements.

Supporting Information Available: ¹H NMR spectrum of 1:1 C₁₂Ala–SDS ion-pair complex in CDCl₃ solvent and the method of determination of the cac of C₁₂Ala including a plot

of surface tension versus log [C₁₂Ala]. This material is available free of charge via the Internet at <http://pubs.acs.org>.

References and Notes

- (1) Moulik, S. P.; Haque, Md. E.; Jana, P. K.; Das, A. R. *J. Phys. Chem.* **1996**, *100*, 701.
- (2) Sharma, K. S.; Patil, S. R.; Rakshit, A. K. *J. Phys. Chem. B* **2004**, *108*, 12804.
- (3) Jana, P. K.; Moulik, S. P. *J. Phys. Chem.* **1991**, *95*, 9525.
- (4) Bury, R.; Triner, C.; Chevalet, C.; Makayssi, A. *Anal. Chim. Acta* **1991**, *251*, 69.
- (5) Makayssi, A.; Bury, R.; Triner, C. *Langmuir* **1994**, *10*, 1359.
- (6) Jacobson, A. M.; Crars, F. J. *J. Colloid Interface Sci.* **1991**, *142*, 480.
- (7) Haque, M. E.; Das, A. R.; Rakshit, A. K.; Moulik, S. P. *Langmuir* **1996**, *12*, 4084.
- (8) Sulthana, S. B.; Rao, P. V. C.; Bhat, S. G. T.; Nakano, T. Y.; Sugihara, G.; Rakshit, A. K. *Langmuir* **2000**, *16*, 980.
- (9) Elkadi, N.; Martins, F.; Clausse, D.; Schulz, P. C. *Colloid Polym. Sci.* **2003**, *281*, 353.
- (10) Castaldi, M. L.; Ortona, O.; Paduano, L.; Vitagliano, V. *Langmuir* **1998**, *14*, 5994.
- (11) Sulthana, S. B.; Rao, P. V. C.; Bhat, S. G. T.; Rakshit, A. K. *J. Phys. Chem. B* **1998**, *102*, 9653.
- (12) Buwalda, R. T.; Jonker, J. M.; Engberts, J. B. F. N. *Langmuir* **1999**, *15*, 1083.
- (13) Buwalda, R. T.; Stuart, M. C. A.; Engberts, J. B. F. N. *Langmuir* **2002**, *18*, 6507.
- (14) Caillet, C.; Hebrant, M.; Tondre, C. *Langmuir* **2000**, *16*, 9099.
- (15) Xia, Y.; Goldmints, I.; Johnson, P. W.; Hatton, T. A.; Bose, A. *Langmuir* **2002**, *18*, 3822.
- (16) Shioi, A.; Hatton, T. A. *Langmuir* **2002**, *18*, 7341.
- (17) Yacilla, M.; Herrington, K. L.; Brasher, L. L.; Kaler, E. W.; Chiruvolu, S.; Zasadzinski, J. A. *J. Phys. Chem.* **1996**, *100*, 5874.
- (18) Chakraborty, H.; Sarkar, M. *Langmuir* **2004**, *20*, 3551.
- (19) Kaler, E. W.; Murthy, A. K.; Rodriguez, B. E.; Zasadzinski, J. A. *N. Science* **1989**, *245*, 1371.
- (20) Kaler, E. W.; Herrington, K. L.; Murthy, A. K.; Zasadzinski, J. A. *N. J. Phys. Chem.* **1992**, *96*, 6698.
- (21) Brasher, L. L.; Herrington, K. L.; Kaler, E. W. *Langmuir* **1995**, *11*, 4267.
- (22) Koehler, R. D.; Raghavan, S. R.; Kaler, E. W. *J. Phys. Chem. B* **2000**, *104*, 11035.
- (23) Schubert, B. A.; Kaler, E. W.; Wagner, N. J. *Langmuir* **2003**, *19*, 4079.
- (24) Limin, Z.; Ganzuo, L.; Zhiwei, S. *Colloid Surf., A* **2001**, *190*, 275.
- (25) Zhai, L.; Zhang, J.; Shi, Q.; Chen, W.; Zhao, M. *J. Colloid Interface Sci.* **2005**, *284*, 698.
- (26) Rosa, M.; Infant, M. R.; Miguel, M. da G.; Lindman, B. *Langmuir* **2006**, *22*, 5588.
- (27) (a) Khatua, D.; Maiti, R.; Dey, J. *J. Chem. Soc., Chem. Commun.* **2006**, 4903. (b) Khatua, D.; Dey, J. *Langmuir* **2005**, *21*, 109.
- (28) Silverstein, R. L.; Webster, F. X. *Spectrometric Identification of Organic Compounds*, 6th Ed.; John Wiley and Sons: New York, 1998.
- (29) Mata, J.; Varade, D.; Ghosh, G.; Bahadur, P. *Colloids Surf., A* **2004**, *245*, 69.
- (30) Pecora, R., Ed. *Dynamic Light Scattering: Applications of Photon Correlation Spectroscopy*; Plenum Press: New York and London, 1985.
- (31) Aswal, V. K.; Goyal, P. S. *Curr. Sci.* **2000**, *79*, 947.
- (32) Rosen, M. J. *Surfactants and Interfacial Phenomena*, 3rd ed.; John Wiley and Sons: New York, 2004.
- (33) Saitoh, T.; Taguchi, K.; Hiraide, M. *Anal. Chim. Acta* **2002**, *454*, 203.
- (34) (a) Kalyanasundaram, K.; Thomas, J. K. *J. Am. Chem. Soc.* **1977**, *99*, 2039. (b) Kalyanasundaram, K. *Photophysics of Microheterogeneous Systems*; Academic Press: New York, 1988.
- (35) Zana, R. In *Surfactant Solutions. New Methods of Investigation*; Zana, R., Ed.; M. Dekker: New York, 1987; Chapter 5.
- (36) Shinitzky, M. In *Physical Methods on Biological Membranes and their Model Systems*; Plenum Publishing Corp.: New York, 1984; p 237.
- (37) Zana, R.; In, M.; Lévy, H. *Langmuir* **1997**, *13*, 5552.
- (38) Roy, S.; Mohanty, A.; Dey, J. *J. Chem. Phys. Lett.* **2005**, *414*, 23.
- (39) (a) Dutt, G. B. *J. Phys. Chem. B* **2004**, *108*, 3651. (b) Kubota, Y.; Kodama, M.; Miura, M. *Bull. Chem. Soc. Jpn.* **1973**, *46*, 100.
- (40) Bendedouch, D.; Chen, S. H.; Koehler, W. C. *J. Phys. Chem.* **1983**, *87*, 2621.
- (41) Clausen, T. M.; Vinson, P. K.; Minter, J. R.; Davis, H. T.; Talmon, Y.; Miller, W. G. *J. Phys. Chem.* **1992**, *90*, 474.
- (42) Kalur, G. C.; Frounfelker, D.; Cipriano, B. H.; Norman, A. I.; Raghavan, S. R. *Langmuir* **2005**, *21*, 10998.

- (43) Angelescu, D.; Khan, A.; Caldararu, H. *Langmuir* **2003**, *19*, 9155.
(44) Zhu, Z.; González, Y. I.; Xu, H.; Kaler, E. W.; Liu, S. *Langmuir* **2006**, *22*, 949.
(45) Angelescu, D.; Khan, A.; Caldaram, H. *Langmuir* **2003**, *19*, 9155.
(46) Negatively stained TEM images are often criticized for possible appearance of artifacts due to the sample preparation procedure. However, in the case of the C₁₂Ala-SDS system, such possibility could be eliminated on the basis of the fact that the micrograph of the solution containing an equivalent amount (10 mM) of pure SDS surfactant did not show such

morphology. Moreover, similar microstructures were also found in the micrograph of a structurally similar surfactant, C₁₂Gly, having glycine as the headgroup.

- (47) Nieh, M.-P.; Harroun, T. A.; Raghunathan, V. A.; Glinka, C. J.; Katsaras, J. *Biophys. J.* **2004**, *86*, 2615.
(48) de Gennes, P. G.; Prost, J. *The Physics of Liquid Crystals*; Oxford University Press: Oxford, U.K., 1993.
(49) Radley, K.; Saupe, A. *Mol. Phys.* **1978**, *35*, 1405.
(50) Yu, L. J.; Saupe, A. *J. Am. Chem. Soc.* **1980**, *102*, 4879.